Interaction-enhanced integer quantum Hall effect in disordered systems

Jun-Hui Zheng,[1] Tao Qin,[1,2] and Walter Hofstetter[1]
[1]*Institut für Theoretische Physik, Goethe-Universität, 60438 Frankfurt/Main, Germany*
[2]*School of Physics and Materials Science, Anhui University, Hefei, Anhui Province 230601, People's Republic of China*

(Received 6 June 2018; revised manuscript received 24 January 2019; published 21 March 2019)

We study transport properties and topological phase transition in two-dimensional interacting disordered systems. We derive the Hall conductance within real-space dynamical mean-field theory, which is quantized and serves as a topological invariant for insulators, even when the energy gap is closed by localized states. In the spinful Harper-Hofstadter-Hatsugai model, in the trivial insulator regime, we find that the repulsive on-site interaction can assist weak disorder to induce the integer quantum Hall effect, while in the topologically nontrivial regime, it impedes Anderson localization. Generally, the interaction broadens the regime of the topological phase in the disordered system.

DOI: 10.1103/PhysRevB.99.125138

I. INTRODUCTION

The quantum Hall effect (QHE) in the presence of interaction and disorder has been of great interest for a long time. Interactions play an essential role in the fractional QHE [1] and disorder is responsible for the existence of the plateaux in the Hall conductance [2–5]. For different models, the perfect quantization of conductance can be violated [6–16] or conversely induced [17–32] by disorder and interaction, respectively. Topological invariants (TIs) are constructed to classify the resulting transport properties [33–35] in systems with bulk energy gaps. General expressions for the invariants of interacting and disordered systems were developed from the perspective of the many-body wave functions (MBWs) [36–39]. Nonetheless, the MBWs can be captured numerically only for a rather small size of the interacting system. Equivalent expressions in terms of the single-particle Green's function were developed thereafter, based on the microscopic theory [40–42], which are numerically accessible even for infinite systems if translational symmetry (TS) is assumed [43].

Disorder destroys TS, which increases the difficulty of studying topological phase transitions in interacting disordered systems. A nonperturbative way of dealing with TIs in systems of this type is rare. Most literature on disordered topological systems treats the interaction within the Hartree-Fock approximation [44], the random-phase approximation [45], or perturbative renormalization-group techniques [46–48]. A nonperturbative treatment with quantum Monte Carlo is limited due to the sign problem [49].

In this paper, we focus on the combined effects of on-site interaction and disorder on a topologically trivial or nontrivial insulator, respectively. For general systems in the absence of TS, we derive the Hall conductance within the real-space dynamical mean-field theory (RDMFT). We name the resulting formula the *generalized Ishikawa-Matsuyama formula* (GIMF) [see Eq. (24)]. In the presence of a bulk energy gap, the GIMF is quantized and serves as a TI. Furthermore, as we will prove, localized states do not contribute to the Hall conductance. Thus the GIMF is still a TI even for systems with gapless bulk spectrum, if all states at the Fermi energy are localized.

Numerically, the Hall conductance is directly evaluated by employing RDMFT for a given disordered sample in a finite-size system. The obtained Hall conductance depends on the realization of the disorder. The statistically averaged Hall conductance is obtained for a sufficiently large number of samples. Our numerical result shows that for the topologically nontrivial regime, the Hall conductance is well quantized and the statistical fluctuations are strongly suppressed. Around the phase-transition point, the gap of the system becomes small, the quantization of the Hall conductance is violated due to the finite-size effect, and the statistical fluctuations of the Hall conductance are also increased. In contrast to statistical dynamical mean-field theory (a simplified version of RDMFT based on an ensemble description of disorder, which is applied in Refs. [50,51] to describe phase transition between Anderson localization, metal phase, and a Mott insulator in strongly correlated disordered lattice systems), the direct calculation of the Hall conductance allows us to differentiate between the topologically trivial and nontrivial insulating phases.

As an example, we calculate the Hall conductance of the spinful Harper-Hofstadter-Hatsugai model (HHHM) on a square lattice with half filling [52]. By tuning the strength of the on-site staggered potential, the system can be initially prepared in a topologically trivial or nontrivial state. Then the on-site interaction and disorder are added to investigate their effects. Using RDMFT, we find that, for a trivial insulator with weak disorder, the repulsive on-site interaction can assist the disorder to smoothen the staggered potential more efficiently, and thus induce the integer QHE. This result is consistent with the effective-medium theory (EMT) we develop for weak disorder and weak interaction cases, in which interaction effects are included within the Born approximation. For a topologically nontrivial insulator, the RDMFT results show that the interaction impedes Anderson localization. In general, the interaction broadens the regime of the topological phase in the disordered system.

The remaining parts of the paper are organized as follows. In Sec. II, we derive the Hall conductance for a disordered system within RDMFT, and confirm that it is quantized for insulating phases. The EMT is also developed for weak disorder and weak interaction. In Sec. III, we numerically calculate the Hall conductance for the spinful Harper-Hofstadter-Hatsugai model by using RDMFT. A short summary is given in Sec. IV.

II. HALL CONDUCTANCE WITHIN DYNAMICAL MEAN-FIELD THEORY

In the following we derive the Hall conductance for systems without TS. The results are derived on a square lattice but can similarly be generalized to any periodic lattice structure. The Hamiltonian is

$$\hat{H} = \hat{H}_0 + \hat{H}_{\text{int}}, \tag{1}$$

where

$$\hat{H}_0 = \sum_{i\alpha,j\gamma} \hat{c}^\dagger_{i\alpha}[H_0]_{i\alpha,j\gamma}\hat{c}_{j\gamma} \tag{2}$$

is the noninteracting part and

$$\hat{H}_{\text{int}} = U\sum_i \hat{n}_{i\uparrow}\hat{n}_{i\downarrow} \tag{3}$$

is the on-site interaction. Here, $\boldsymbol{i}$ and $\boldsymbol{j}$ are the lattice indices. α and γ are spin indices. The noninteracting Hamiltonian still contains two parts,

$$\hat{H}_0 = \hat{h}_0 + \hat{H}_{\text{dis}}, \tag{4}$$

where

$$\hat{h}_0 = \sum_{i\alpha,j\gamma} \hat{c}^\dagger_{i\alpha}[h_0]_{i\alpha,j\gamma}\hat{c}_{j\gamma} \tag{5}$$

is the translationally invariant part and $\hat{H}_{\text{dis}}$ represents disorder. Note that $\hat{H}_0$ is not diagonal in momentum space since momentum is not a good quantum number anymore for disordered systems. We denote its matrix elements in momentum space as $H_0(\boldsymbol{k}_1\alpha, \boldsymbol{k}_2\gamma) \equiv [H_0]_{\boldsymbol{k}_1\alpha,\boldsymbol{k}_2\gamma}$.

A. Current operators from the continuity equation

Current operators (COs) can be derived from the continuity equation and the equation of motion of the local-density operator [53]. In the Heisenberg picture, the continuity equation for the particle current is [53]

$$\dot{\hat{\rho}}(\boldsymbol{r},t) + \nabla\cdot\hat{\boldsymbol{J}}(\boldsymbol{r},t) = 0. \tag{6}$$

After Fourier transformation this becomes $\dot{\hat{\rho}}_{\boldsymbol{q}} - i\boldsymbol{q}\cdot\hat{\boldsymbol{J}}_{\boldsymbol{q}} = 0$. For a lattice structure, using the local-density operator $\hat{\rho}_i = \sum_\alpha \hat{c}^\dagger_{i\alpha}\hat{c}_{i\alpha}$, we obtain $\hat{\rho}_{\boldsymbol{q}} = \frac{1}{\sqrt{N}}\sum_{\boldsymbol{k}} \hat{c}^\dagger_{(\boldsymbol{k}+\boldsymbol{q})\alpha}\hat{c}_{\boldsymbol{k}\alpha}$. By using the equation of motion for the density operator, the continuity equation yields

$$-\boldsymbol{q}\cdot\hat{\boldsymbol{J}}_{\boldsymbol{q}} = i\dot{\hat{\rho}}_{\boldsymbol{q}} = [\hat{\rho}_{\boldsymbol{q}}, \hat{H}]. \tag{7}$$

Since the on-site interaction term is locally particle-number conserving, it is easy to check $[\hat{\rho}_i, \hat{H}_{\text{int}}] = 0$. For the noninteracting part, we have

$$\begin{aligned}[\hat{\rho}_{\boldsymbol{q}}, \hat{H}_0] &= \frac{1}{\sqrt{N}}\sum_{\boldsymbol{k}_1\alpha,\boldsymbol{k}_2\gamma}[H_0]_{\boldsymbol{k}_1\alpha,\boldsymbol{k}_2\gamma}\{\hat{c}^\dagger_{(\boldsymbol{k}_1+\boldsymbol{q})\alpha}\hat{c}_{\boldsymbol{k}_2\gamma} - \hat{c}^\dagger_{\boldsymbol{k}_1\alpha}\hat{c}_{(\boldsymbol{k}_2-\boldsymbol{q})\gamma}\} \\ &= \frac{1}{\sqrt{N}}\sum_{\boldsymbol{k}_1\alpha,\boldsymbol{k}_2\gamma}\{[H_0]_{(\boldsymbol{k}_1-\boldsymbol{q}/2)\alpha,(\boldsymbol{k}_2-\boldsymbol{q}/2)\gamma} \\ &\quad - [H_0]_{(\boldsymbol{k}_1+\boldsymbol{q}/2)\alpha,(\boldsymbol{k}_2+\boldsymbol{q}/2)\gamma}\}\hat{c}^\dagger_{(\boldsymbol{k}_1+\boldsymbol{q}/2)\alpha}\hat{c}_{(\boldsymbol{k}_2-\boldsymbol{q}/2)\gamma}. \end{aligned} \tag{8}$$

Thus, from Eqs. (7) and (8), we obtain each component of the current operator,

$$\hat{J}^\mu_{\boldsymbol{q}} = \sum_{\boldsymbol{k}_1\alpha,\boldsymbol{k}_2\gamma}\hat{c}^\dagger_{(\boldsymbol{k}_1+\boldsymbol{q}/2)\alpha}[j^\mu]_{\boldsymbol{k}_1\alpha,\boldsymbol{k}_2\gamma}\hat{c}_{(\boldsymbol{k}_2-\boldsymbol{q}/2)\gamma}, \tag{9}$$

for $\boldsymbol{q}\to\boldsymbol{0}$, where

$$[j^\mu]_{\boldsymbol{k}_1\alpha,\boldsymbol{k}_2\gamma} = \frac{1}{\sqrt{N}}[\bar{\partial}_{k_\mu}H_0]_{\boldsymbol{k}_1\alpha,\boldsymbol{k}_2\gamma}. \tag{10}$$

Here, $[\bar{\partial}_{k_\mu}A]_{\boldsymbol{k}_1\alpha,\boldsymbol{k}_2\gamma} \equiv (\partial_{k_{1\mu}} + \partial_{k_{2\mu}})A(\boldsymbol{k}_1\alpha, \boldsymbol{k}_2\gamma)$ for any matrix A and $\mu = x, y$. N is the total number of lattice sites. We set $\hbar = e = a = 1$, where $\hbar$ is the Planck constant, a is the lattice constant, and e is the electron charge. The CO is the sum of the first derivatives of H_0 with respect to the two momenta. The formula (9) is a generalized CO for any disordered system. From Eq. (9), we can find that the on-site disorder potential does not contribute to the CO, but disordered tunneling terms do. For the system with TS, the Hamiltonian becomes diagonal in momentum space and the CO recovers its ordinary form [53].

B. Hall conductance

The Kubo formula for the dc Hall conductance is [54]

$$\sigma_H = \lim_{\omega\to0}\frac{1}{\omega}\text{Im}\,\Pi_{yx}(i\omega_n\to\omega+i0^+), \tag{11}$$

where the current-current correlation function is

$$\Pi_{yx}(i\omega_n) = \lim_{\boldsymbol{q}\to\boldsymbol{0}}\int_0^\beta d\tau e^{i\omega_n\tau}\langle T_\tau\hat{J}^y_{\boldsymbol{q}}(\tau)\hat{J}^x_{-\boldsymbol{q}}(0)\rangle. \tag{12}$$

Using l'Hôpital's rule and the Cauchy-Riemann equations, we have

$$\sigma_H = \partial_{\omega_x}\text{Im}\,\Pi_{yx}(z)|_{z=i0^+} = -\partial_{\omega_y}\text{Re}\,\Pi_{yx}(z)|_{z=i0^+}, \tag{13}$$

where $z = \omega_x + i\omega_y$. So the dc Hall conductivity becomes

$$\sigma_H = -\partial_\omega\text{Re}\,\Pi_{yx}(i\omega)|_{\omega=0^+}. \tag{14}$$

1. Without vertex correction

Without considering the quantum correction to the vertex, the current-current correlation function becomes

$$\Pi_{yx} = \frac{1}{\beta}\sum_{n'}\text{Tr}[j^yG(i\omega_{n'}+i\omega_n)j^xG(i\omega_{n'})], \tag{15}$$

where the trace is for both momentum and spin degree of freedom. Note that in RDMFT, only the on-site self-energy is taken into account in the Green's function [43,55],

$$\Sigma_{i\alpha,j\gamma}(i\omega) = \Sigma_{i\alpha,i\gamma}(i\omega)\delta_{ij}. \tag{16}$$

After Fourier transformation to momentum space, we find $[\bar{\partial}_{k_\mu}\Sigma]_{\boldsymbol{k}_1\alpha,\boldsymbol{k}_2\gamma}=0$. By using the fact

$$G^{-1}_{i\omega}=i\omega\mathbf{1}-H_0-\Sigma_{i\omega}, \tag{17}$$

we have

$$j^\mu=-\frac{1}{\sqrt{N}}\bar{\partial}_{k_\mu}G^{-1}_{i\omega} \tag{18}$$

within RDMFT. Thus the correlation function (12) becomes

$$\Pi_{yx}(i\omega_n)=\frac{1}{N\beta}\sum_{n'}\mathrm{Tr}[\bar{\partial}_{k_y}G^{-1}(i\omega_{n'})G(i\omega_{n'}+i\omega_n)\times\bar{\partial}_{k_x}G^{-1}(i\omega_{n'})G(i\omega_{n'})]. \tag{19}$$

In the zero-temperature limit, we can use the replacement $\frac{1}{\beta}\sum_{n'}\to\int\frac{d\omega}{2\pi}$, and thus the summation becomes an integral. In addition, using the fact that $\partial_\omega G=-G\partial_\omega G^{-1}G$, we obtain

$$\begin{aligned}F_{\mu\nu}&\equiv-\partial_\omega\Pi_{\mu\nu}(i\omega)|_{\omega=0^+}\\&=\frac{1}{2\pi N}\int d\omega\mathrm{Tr}[G_{i\omega}\bar{\partial}_{k_\mu}G^{-1}_{i\omega}G_{i\omega}\partial_\omega G^{-1}_{i\omega}G_{i\omega}\bar{\partial}_{k_\nu}G^{-1}_{i\omega}],\end{aligned} \tag{20}$$

for $\mu,\nu=x,y$. Note that the Hall conductance is defined as $\sigma_H=\mathrm{Re}\,F_{yx}=(F_{yx}+F^*_{yx})/2$. From the Lehmann representation, we can find that the Green's function satisfies the following relation:

$$\left(G^{-1}_{i\omega}\right)^*=\left(G^{-1}_{-i\omega}\right)^T, \tag{21}$$

where T means transpose. It implies

$$\left(\bar{\partial}_{k_\mu}G^{-1}_{i\omega}\right)^*=\bar{\partial}_{k_\mu}\left(G^{-1}_{-i\omega}\right)^T=\bar{\partial}_{k_\mu}\left(G^{-1}_{i\tilde{\omega}}\right)^T\big|_{\tilde{\omega}=-\omega}, \tag{22}$$

$$\left(\partial_\omega G^{-1}_{i\omega}\right)^*=\partial_\omega\left(G^{-1}_{-i\omega}\right)^T=-\partial_{\tilde{\omega}}\left(G^{-1}_{i\tilde{\omega}}\right)^T\big|_{\tilde{\omega}=-\omega}. \tag{23}$$

Using the fact that a matrix and its transpose have the same trace, we can obtain $\sigma_H=(F_{yx}-F_{xy})/2$. Since the trace is invariant under cyclic permutations, the Hall conductance in the zero-temperature limit becomes $\sigma_H=\chi/2\pi$, where

$$\chi\equiv\frac{\epsilon^{\tilde{\mu}\tilde{\nu}\tilde{\rho}}}{6N}\int d\omega\mathrm{Tr}\left[G_{i\omega}\left(\bar{\partial}_{\tilde{\mu}}G^{-1}_{i\omega}\right)G_{i\omega}\left(\bar{\partial}_{\tilde{\nu}}G^{-1}_{i\omega}\right)G_{i\omega}\left(\bar{\partial}_{\tilde{\rho}}G^{-1}_{i\omega}\right)\right]. \tag{24}$$

The indices $\tilde{\mu}$, $\tilde{\nu}$, and $\tilde{\rho}$ run through k_x, k_y, and ω, and $[\bar{\partial}_\omega G_{i\omega}]_{\boldsymbol{k}_1\alpha,\boldsymbol{k}_2\gamma}\equiv\partial_\omega G_{i\omega}(\boldsymbol{k}_1\alpha,\boldsymbol{k}_2\gamma)$. We denote the quantity χ as GIMF. The GIMF reduces to the original formula [40] when the TS is recovered.

2. *Quantum correction for the vertex*

In the above, the quantum correction for the vertex is excluded. Actually, within RDMFT, the contribution from the vertex corrections of the CO to the Hall conductance is suppressed by the dimensionality of the system in the absence of disorder [43,56]. In Appendix C, we show that in the presence of disorder, using the Ward-Takahashi identity, the vertex at the long-wave limit (i.e., with a long-wave and zero mode photon as an external leg) is $-\frac{1}{\sqrt{N}}\bar{\partial}_{k_\mu}G^{-1}_{i\omega}$, with full quantum corrections. In RDMFT, this quantity is exactly the same as the bare vertex, i.e., $\frac{1}{\sqrt{N}}\bar{\partial}_{k_\mu}G^{-1}_{i\omega}=\frac{1}{\sqrt{N}}\bar{\partial}_{k_\mu}G^{-1}_{0,i\omega}$, where $G^{-1}_{0,i\omega}=i\omega\mathbf{1}-H_0$ is the inverse of the free Green's function. Therefore Eq. (24) exactly represents the Hall conductance within the approximation of RDMFT. To obtain a better expression for the Hall conductance, one has to go beyond the single-site dynamical mean-field theory and apply the cluster dynamical mean-field theory to include the nonlocal self-energies $\Sigma_{\boldsymbol{i}\alpha,\boldsymbol{j}\gamma}(i\omega)$ with $\boldsymbol{i}\neq\boldsymbol{j}$ [57]. The nonlocal selfenergies contribute quantum corrections to the hopping terms and also the current operators, which will not be discussed here.

3. *Properties of* χ

An important result for Eq. (24) is that *the GIMF* χ *is quantized and serves as a TI for insulators, regardless of whether the bulk spectrum is gapped or gapless.* The result is evident for gapped cases (see Appendix A). However, for disordered systems, the gap can be closed by disorder. The system can still be an insulator, but with all of the states at the Fermi energy being localized. In next subsection, we will illustrate that none of the localized states contributes to the conductance. Thus, the Hall conductance is unchanged and still quantized when these localized states cross through the Fermi energy.

C. Numerical realization

The above Hall conductivity is derived in the thermodynamic limit. In the numerical approach, the sample for the disorder configuration can be realized only for a finite size system (FSS) with $n_x\times n_y$ lattices. To apply Eq. (24) to the disordered system, we construct an extended infinite system (EIS), by periodically repeating the FSS in space [58]. The EIS is a quasidisordered system. The real disordered system can be approached when n_x and n_y become large. The idea is equivalent to introducing twisted boundary conditions to the FSS. In the EIS, the system again becomes periodic in the real space, in which the FSS is a supercell [58,59]. In the first Brillouin zone, the Bloch wave vector is $\boldsymbol{\theta}\equiv(\theta_x,\theta_y)$ with $\theta_\mu\in[0,2\pi/n_\mu)$ for $\mu=x,y$. Each supercell has $2n_xn_y$ internal degrees of freedom, where the factor 2 is contributed by the spin. The position $\boldsymbol{i}$ in the EIS can be expressed as $\boldsymbol{i}=\boldsymbol{R}+\boldsymbol{r}$, where $\boldsymbol{R}$ is the position of the corresponding supercell and $\boldsymbol{r}$ is the relative position in the supercell.

We define the twisted matrix $A^{\boldsymbol{\theta}}$ as follows:

$$A^{\boldsymbol{\theta}}_{\boldsymbol{r}\alpha,\boldsymbol{r}'\gamma}\equiv\sum_{\boldsymbol{R}}A_{(\boldsymbol{R}+\boldsymbol{r})\alpha,\boldsymbol{r}'\gamma}\exp[i\boldsymbol{\theta}\cdot(\boldsymbol{R}+\boldsymbol{r}-\boldsymbol{r}')], \tag{25}$$

for a general matrix A in real space. We find that $\Sigma^{\boldsymbol{\theta}}_{i\omega}=\Sigma_{i\omega}$ and $G^{\boldsymbol{\theta}}_{i\omega}=1/(i\omega\mathbf{1}-H^{\boldsymbol{\theta}}_0-\Sigma_{i\omega})$, with $\mathbf{1}$ being the identity matrix. Then, the GIMF can be rewritten as

$$\chi=\frac{\epsilon^{\tilde{\mu}\tilde{\nu}}}{8\pi^2}\int d\omega d\boldsymbol{\theta}\mathrm{Tr}\left[\left(\partial_{\tilde{\mu}}H^{\boldsymbol{\theta}}_0\right)G^{\boldsymbol{\theta}}_{i\omega}\left(\partial_{\tilde{\nu}}H^{\boldsymbol{\theta}}_0\right)G^{\boldsymbol{\theta}}_{i\omega}A_{i\omega}G^{\boldsymbol{\theta}}_{i\omega}\right], \tag{26}$$

where $\tilde{\mu}$ and $\tilde{\nu}$ run through θ_x and θ_y now, and $A_{i\omega}=i\mathbf{1}-\partial_\omega\Sigma_{i\omega}$. A detailed derivation can be found in Appendix B. Equation (26) is exactly the first Chern number of a periodic system with the Bloch momentum $\boldsymbol{\theta}$, in which the sites in the supercell are treated as internal degrees of freedom, i.e., a pseudospin. The method is consistent with the proposal of a topological index in a disordered system via introducing twisted phases for the Green's function [41].

1. Contribution from local states

Now we illustrate that the localized states do not contribute to the Hall conductance. Following the contour-integration method developed in Refs. [60] and [61], Eq. (26) can be expressed by the summation of the Berry curvature of all occupied quasiparticle states. The GIMF becomes

$$\chi = \sum_{\text{occu.}} \frac{\varepsilon^{\tilde{\mu}\tilde{\nu}}}{2\pi i} \int d^2\boldsymbol{\theta} \langle \partial_{\tilde{\mu}} \psi^{\boldsymbol{\theta}} | \partial_{\tilde{\nu}} \psi^{\boldsymbol{\theta}} \rangle. \tag{27}$$

Here, the quasiparticle state $\psi^{\boldsymbol{\theta}}$ is the eigenstate of $G_\omega^{\boldsymbol{\theta}}$ at its pole for real frequencies. It is also the eigenvector of $\omega\mathbf{1} - H_0^{\boldsymbol{\theta}} - \Sigma_\omega$ at the zeros. By varying the twisted phase, we obtain quasiparticle bands in $\boldsymbol{\theta}$ space. Let us suppose that the size of the supercell is significantly larger than the localization length. Considering a localized state ψ for $\boldsymbol{\theta} = 0$, we can shift the position of the supercell so that the localized state is almost in the center of the supercell and thus ψ vanishes away from the center. Note that the difference between $\omega\mathbf{1} - H_0^{\boldsymbol{\theta}} - \Sigma_\omega$ and $\omega\mathbf{1} - H_0^{\boldsymbol{\theta}=0} - \Sigma_\omega$ is only the unitary transformation $e^{i\boldsymbol{\theta}\cdot\boldsymbol{r}}$ besides the elements near the edge of the supercell. Then for a localized state, the twisted boundary condition does not change the position of the pole of the Green's function and the corresponding eigenstate apart from a unitary transformation, since the eigenstate vanishes at the boundary if we properly choose the position of the edge of the supercell. For the localized state, the difference at the edge of the supercell has no effect, and thus $\psi^{\boldsymbol{\theta}} = e^{i\boldsymbol{\theta}\cdot\boldsymbol{r}}\psi^{\boldsymbol{\theta}=0}$. A localized state forms a flat band upon varying the twisted phase and the corresponding Berry curvature is always trivial by substituting $\psi^{\boldsymbol{\theta}}$ into Eq. (27). This implies that localized states do not contribute to the conductance. The Hall conductance is still quantized regardless of whether these localized states (bands) cross through the Fermi energy.

2. RDMFT

The self-energy in the Green's function can be obtained by using RDMFT [55] for each disorder configuration in a FSS. Within this approach, the system is mapped to a set of coupled single impurity problems, where the other sites, acting as a bath, are integrated out. The effective action for each single impurity is $S_{\boldsymbol{i}} = -\int d\tau d\tau' c^\dagger(\tau)\mathcal{G}_{0,\boldsymbol{i}}^{-1}(\tau - \tau')c(\tau') + U\int d\tau n_{\boldsymbol{i}\downarrow} n_{\boldsymbol{i}\uparrow}$, where $\mathcal{G}_{0,\boldsymbol{i}}$ is the Weiss function at the site $\boldsymbol{i}$ and the spin indices are hidden [43]. The full Green's function is given by the Dyson equation, $\mathcal{G}_{\boldsymbol{i}}^{-1}(i\omega_n) = \mathcal{G}_{0,\boldsymbol{i}}^{-1}(i\omega_n) - \Sigma_{\boldsymbol{ii}}(i\omega_n)$, where each term depends on the site $\boldsymbol{i}$ in the supercell. We use iterative perturbation theory to obtain the self-energy for each single impurity problem [62,63]. The full lattice Green's function is given by $G(i\omega_n) = 1/(i\omega_n\mathbf{1} - H_0 - \Sigma)$. A self-consistent solution is found by closing the loop with $\mathcal{G}_{\boldsymbol{i}} = G_{\boldsymbol{ii}}$.

D. Effective-medium theory for weak disorder and weak interaction limit

In this subsection, we show the EMT for the case of weak disorder and interaction. It is a perturbative mean-field method, in which the effective Hamiltonian $H_{\text{eff}} \equiv h_0 + \overline{\Sigma}$ obtains a translationally invariant form. The self-energy is the statistically averaged result over different disorder samples. Specifically, we focus on a system with an on-site potential $\hat{H}_{\text{dis}} = \sum_{i\alpha} V_i \hat{n}_{i\alpha}$, where V_i is random and position dependent but uniformly distributed in $[-W, W]$. The self-energy is defined through the expression $\overline{G} = 1/(\omega\mathbf{1} - h_0 - \overline{\Sigma})$ at $\omega = 0$, where $\overline{G}$ is the disorder-averaged Green's function. As we prove in Appendix D, the self-energy, up to the order of W^2 and U, is given by

$$\overline{\Sigma}_{i\alpha,i\gamma} = \overline{\Sigma}^{\text{dis}}_{i\alpha,i\gamma} + \overline{\Sigma}^{\text{U}}_{i\alpha,i\gamma}, \tag{28}$$

where $\overline{\Sigma}^{\text{dis}}_{i\alpha,i\gamma} = W^2\overline{G}_{i\alpha,i\gamma}/3$ is contributed by the disorder [23] and $\overline{\Sigma}^{U}_{i\alpha,i\gamma}$ is the statistical average of the Hartree-Fock self-energy $U\langle\hat{c}_{i\alpha}\hat{c}^\dagger_{i\bar{\alpha}}\rangle\delta_{\bar{\alpha}\gamma} + U\langle\hat{c}^\dagger_{i\bar{\alpha}}\hat{c}_{i\bar{\alpha}}\rangle\delta_{\alpha\gamma}$ with $\bar{\uparrow} = \downarrow$ and $\bar{\downarrow} = \uparrow$. The statistical expectation values of the local operators $\hat{c}_{i\alpha}\hat{c}^\dagger_{i\bar{\alpha}}$ and $\hat{c}^\dagger_{i\bar{\alpha}}\hat{c}_{i\bar{\alpha}}$ can be calculated through the effective Hamiltonian H_{eff}. Thus the self-energy can be solved self-consistently. Note that this EMT cannot predict Anderson localization. It only describes the contribution of the extended states. Later, we will see that the self-energy $\overline{\Sigma}$ can effectively describe the band inversion due to weak interaction and weak disorder.

III. SPINFUL HARPER-HOFSTADTER-HATSUGAI MODEL

Now, we consider the HHHM on the square lattice [52]. The translationally invariant part of the Hamiltonian is

$$\begin{aligned}\hat{h}_0 = &-\sum_{\boldsymbol{i},\alpha}[t_x\hat{c}^\dagger_{\boldsymbol{i}+\hat{x},\alpha}\hat{c}_{\boldsymbol{i}\alpha} + t_y e^{i2\pi\xi i_x}\hat{c}^\dagger_{\boldsymbol{i}+\hat{y},\alpha}\hat{c}_{\boldsymbol{i}\alpha} + \text{H.c.}] \\ &- \sum_{\boldsymbol{i},\alpha} t_z[e^{i2\pi\xi(i_x+1/2)}(\hat{c}^\dagger_{\boldsymbol{i}+\hat{x}+\hat{y},\alpha}\hat{c}_{\boldsymbol{i}\alpha} + \hat{c}^\dagger_{\boldsymbol{i}+\hat{y},\alpha}\hat{c}_{\boldsymbol{i}+\hat{x},\alpha}) + \text{H.c.}] \\ &+ \sum_{\boldsymbol{i},\alpha}[(-1)^{i_x}\Lambda - \mu_0]\hat{n}_{\boldsymbol{i}\alpha}.\end{aligned} \tag{29}$$

Here, t_x and t_y are the nearest-neighbor hopping along the x and y direction respectively, t_z is the next-nearest-neighbor hopping, μ_0 is the chemical potential determined by the filling, $\hat{x} = (1, 0)$ and $\hat{y} = (0, 1)$ are the unit vectors, and $\boldsymbol{i} = (i_x, i_y)$. We focus on the case with $\xi = 1/2$, in which there is a π flux in each unit square. The total particle number is fixed to be N, so that the average filling is $1/2$.

Without disorder and interaction, since the spin is conserved and due to the SU(2) symmetry in spin space, the Hamiltonian becomes $h_0 = \boldsymbol{v}(\boldsymbol{k})\cdot\boldsymbol{\sigma} - \mu_0$ in momentum space. Here, $\boldsymbol{v}(\boldsymbol{k}) = -(2t_x\cos k_x, 4t_z\sin k_y\sin k_x, \Lambda - 2t_y\cos k_y)$ is the Bloch vector and $\boldsymbol{\sigma}$ are the Pauli matrices in the pseudospin corresponding to the odd (up) and even (down) position along the x axis. The identity matrices in spin and pseudospin spaces are omitted. For $|\Lambda| < 2t_y$, the Bloch vector covers the origin, and thus, the system is a topological insulator. Increasing the staggered potential, the system closes the band gap at $|\Lambda| = 2t_y$; it becomes a trivial insulator thereafter.

A. Weak disorder and weak interaction case (EMT)

For the weakly disordered and interacting case, we give a discussion based on the EMT for the HHHM. In the EMT, the effective Hamiltonian is $H_{\text{eff}} = h_0 + \overline{\Sigma}$, where $\overline{\Sigma} = \overline{\Sigma}_0 + \overline{\Sigma}_z\sigma_z$. For the half filling case, with a small but finite

temperature, we have $\mu_0 = \overline{\Sigma}_0$ due to the particle-hole symmetry. Thus, the effective Hamiltonian becomes $H_{\rm eff} = \boldsymbol{d}\cdot\boldsymbol{\sigma}$, where $d_x = \boldsymbol{v}_x$, $d_y = \boldsymbol{v}_y$, and $d_z = \boldsymbol{v}_z + \overline{\Sigma}_z$. From the EMT, we get $\overline{\Sigma}^{\rm dis} = -\frac{W^2}{12\pi^2}\int d^2\boldsymbol{k}\frac{d_z\sigma_z}{|\boldsymbol{d}|^2}$ and $\overline{\Sigma}^{\rm U} = \frac{U}{2}(n_{\rm o}+n_{\rm e}) + \frac{U}{2}(n_{\rm o}-n_{\rm e})\sigma_z$, where $n_{\rm o}$ and $n_{\rm e}$ are the particle number for each spin at the odd and the even position along the x axis. The integral region is $k_x, k_y \in [0, 2\pi]$, which is the doubling of the Brillouin zone (one can also use the first Brillouin zone as the integral region, then the coefficient in front of the integral becomes twice as large accordingly). The Fock term does not appear in $\overline{\Sigma}^{\rm U}$ since the spin is conserved. At half filling, for each spin, we have $n_{\rm o}+n_{\rm e}=1$. Note that $n_{\rm o}-n_{\rm e} = \langle\sigma_z\rangle$ is the pseudospin polarization. Thus, we obtain the chemical potential $\mu_0 = U/2$ and the self-consistent self-energy

$$\overline{\Sigma} = \frac{U}{2} - \left\{\frac{W^2}{12\pi^2}\int d^2\boldsymbol{k}\frac{d_z}{|\boldsymbol{d}|^2} + \frac{U}{8\pi^2}\int d^2\boldsymbol{k}\frac{d_z}{|\boldsymbol{d}|}\right\}\sigma_z. \quad (30)$$

As an approximation, one can use $\boldsymbol{v}$ to replace $\boldsymbol{d}$ in the integral above. The effective staggered potential in $H_{\rm eff}$ then becomes $\Lambda_{\rm eff} = (1-\kappa)\Lambda$, where $\kappa\Lambda = -\frac{W^2}{12\pi^2}\int d^2\boldsymbol{k}\frac{\boldsymbol{v}_z}{|\boldsymbol{v}|^2} - \frac{U}{8\pi^2}\int d^2\boldsymbol{k}\frac{\boldsymbol{v}_z}{|\boldsymbol{v}|}$. Independently of the sign of Λ, we find $\kappa > 0$, which means that the weak disorder and interaction effectively smoothen the staggered potential. Intuitively, one would expect that the disorder may randomly intensify or weaken the staggering. However, states are preferably localized around those positions where the staggered potential has been increased. Thus for the extended states, which contribute to the conductance, the effective staggered potential becomes smooth. In addition, the repulsive interaction prefers to induce a uniform distribution of particles in space. This explains why the interaction assists the disorder in decreasing the effective staggered potential.

B. General case (RDMFT)

For the general case of arbitrary interaction and disorder strengths, we use RDMFT to describe interaction effects. In Figs. 1 and 2, we show our numerical results for the case $n_x = n_y = 24$. For simplicity, we choose parameters $t_x = t_y = t_z = t$ and $k_BT = t/40$. The grid for the twisted phase $\boldsymbol{\theta}$ is 8×8. For each value of U and W, we generate 5–100 sample realizations of the disorder. We also assume that the SU(2) symmetry holds for the spin components for weak and moderate interaction. The final Hall conductance is obtained by averaging the Hall conductance over these samples. Numerically, deviations of the obtained conductance from the quantized value are mainly due to finite-size effects and partially due to finite-temperature effects.

In Fig. 1, we show the RDMFT results for the Hall conductance for a system without staggered potential. For $W = U = 0$, the system is a topological insulator. In the EMT, the effective Hamiltonian is not changed by interaction and disorder, i.e., $\Lambda_{\rm eff} = \Lambda = 0$. This means that no band inversion occurs and no topological phase transition is predicted in EMT. However, disorder broadens the distribution of the spectrum in each of the two bands. The marginal states of each band become localized. In the RDMFT calculation, by increasing the disorder strength, the Hall conductance, as a TI, is well quantized before the gap is closed. Thereafter the Hall conductance decreases when further increasing the disorder. As illustrated in Ref. [23], for strong disorder, the topological phase transition follows a localization transition. From Fig. 1, we observe that the interaction effectively impedes the closing

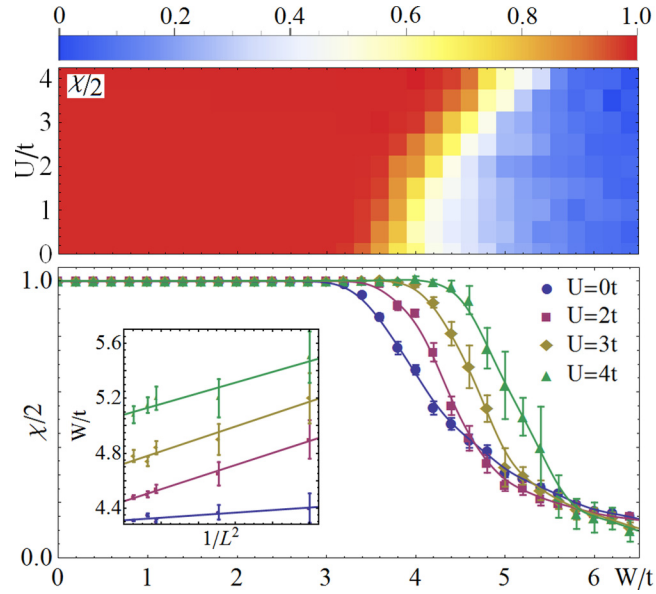

FIG. 1. The density plot (upper) and error list plot (lower) of $\chi/2$ as a function of disorder strength and interaction strength, for $\Lambda = 0$. The inset shows the disorder strength where $\chi/2 = 0.5$, as a function of $1/L^2$ and for different interaction strengths, where L^2 is the size of the supercell with $n_x = n_y = L$ (from left to right: $L = 44, 28, 24, 14, 10$).

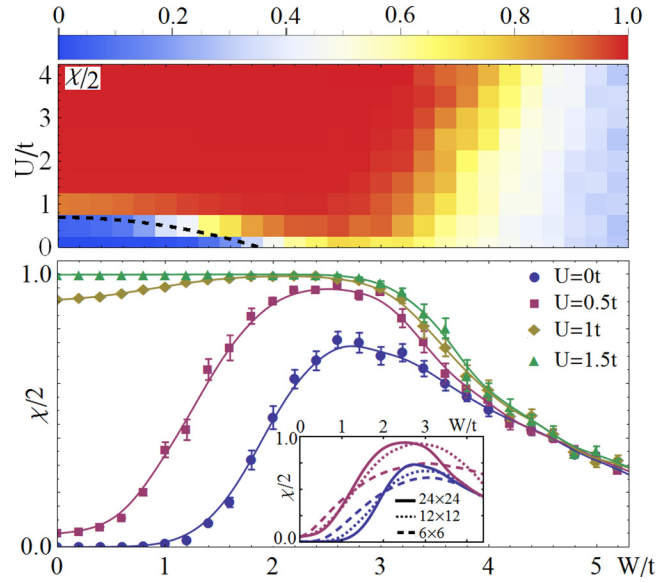

FIG. 2. The density plot (upper) and error list plot (lower) of $\chi/2$ as a function of disorder strength and interaction strength, for $\Lambda = 2.2t$. The dashed black line shown in the upper figure is given by the EMT; see Eq. (30). The inset in the lower figure shows how the value of $\chi/2$ depends on the size of supercell, where the blue (red) lines are for $U = 0.0t$ $(0.5t)$.

of gap and the subsequent topological phase transition and Anderson localization. This shows the fact that the repulsive on-site interaction effectively smoothens the disordered potential. To get rid of the finite size effect, in the inset, we also plot the critical disorder strength (where $\chi/2 = 0.5$) as a function of $1/L^2$ and for different interaction strengths, where $n_x = n_y = L$ is the size of the supercell. The scaling behavior shows an approximately linear dependence of the critical disorder strength on $1/L^2$. The vertical intercepts of these lines represent the critical disorder strength of the topological phase transition in the thermodynamic limit for different interaction strength. The vertical intercept is monotonically increasing with respect to the interaction strength, which again confirms that topological phase transition is impeded by the interaction.

In Fig. 2, we show the RDMFT result of the Hall conductance for $\Lambda = 2.2t$. The system is a topologically trivial insulator for $W = U = 0$. For weak disorder and weak interaction, both increasing the disorder strength and increasing the interaction strength will raise the Hall conductance. From EMT we know that the repulsive on-site interaction can assist the disorder to smoothen the large staggered potential more effectively, and induce the integer quantum Hall effect through band inversion, which occurs at $\Lambda_{\text{eff}} = 2.0t$. Comparing with the RDMFT results, the EMT gives an accurate prediction for the topological phase-transition line for weak disorder and interaction (see the dashed black line shown in the density plot of $\chi/2$ in Fig. 2). When disorder becomes stronger, the Hall conductance decreases again. The interaction also impedes formation of Anderson localization through many-body effects. In the inset, we show $\chi/2$ for different sizes of the supercell. The intersection points of different curves approximately predict the location of the phase transition. From the inset, we observe that the phase transition is located around $W = 2.0t$ for $U = 0$ and around $W = 1.0t$ for $U = 0.5t$, which is really close to the predictions from the EMT. Note the EMT is limited. The effective Hamiltonian is translationally invariant. Thus it is an effective description only for the extended states. It cannot predict the Anderson localization of the system with strong disorder.

In both cases, the interaction broadens the regime of the topological phase in the disordered system. The interaction effectively smoothens the staggered potential and has a delocalizing effect. The prediction from EMT deviates from the RDMFT results when disorder becomes large. The delocalization due to interaction is also observed in topologically trivial systems [50,51,64–66]. We attribute this effect to the following two facts. The repulsive interaction prefers to induce a uniform distribution of particles in space for minimizing the energy, which impedes the formation of localized states. On the other hand, given the localized states in a noninteracting system, the interactions enhance the coupling between them. These "island" states are thus delocalized, provided that the "electron" becomes itinerant between these states.

In the current numerical calculation, we have assumed that the SU(2) symmetry still holds for the spin components for weak and moderate interaction strength. This is not true when the interaction strength becomes stronger, where the system goes into a magnetization regime [21].

Note that the corresponding one-dimensional model after the dimensional reduction of the HHHM is the Rice-Mele model, the Thouless pumping of which has been observed in experiments for both bosonic and fermionic systems [67,68]. This method can be used to measure the Hall coefficient in the absence of disorder. In electronic condensed matter, quenched disorder is generically present [48], and in cold atom systems it can be realized by creating an optical speckle potential through a holographic diffuser [66,69–73]. Recently, the nonzero winding number of the disordered Su-Schrieffer-Heeger model has been observed by measuring the chiral displacement, identifying the one-dimensional topological Anderson insulator [74]. On the other hand, the Chern number of the Harper-Hofstadter model has also been measured through the transverse deflection of an atomic cloud in response to an optical gradient [75]. For the HHHM, only an additional next-nearest-neighbor hopping is needed. In combination with the speckle-induced disorder, it should be realizable in experiments in the foreseeable future.

IV. SUMMARY

In summary, we have generalized the Ishikawa-Matsuyama formula for the topological index to systems without translational invariance and calculated the Hall conductance for a lattice system in the presence of disorder by using RDMFT. The combined effect of interaction and disorder is discussed. We find that the integer quantum Hall effect is enhanced by the on-site interaction for disordered systems.

ACKNOWLEDGMENTS

J.-H. Zheng would like to thank L. Jiang and B. Irsigler for careful reading of the draft. This work was supported by the Deutsche Forschungsgemeinschaft (DFG, German Research Foundation) under Project No. 277974659 via Research Unit FOR 2414.

APPENDIX A: HALL CONDUCTANCE AS A TOPOLOGICAL INDEX FOR GAPED SYSTEMS

For any two matrices A and B in $\boldsymbol{k}$ space, according to our convention, we have

$$[\bar{\partial}_{k_\mu}(AB)]_{\boldsymbol{k}_1,\boldsymbol{k}_2} = (\partial_{k_{1,\mu}} + \partial_{k_{2,\mu}}) \sum_{\boldsymbol{k}_3} A(\boldsymbol{k}_1, \boldsymbol{k}_3) B(\boldsymbol{k}_3, \boldsymbol{k}_2). \quad \text{(A1)}$$

In addition, we also have

$$\sum_{\boldsymbol{k}_3} \partial_{k_{3,\mu}} \{A(\boldsymbol{k}_1, \boldsymbol{k}_3) B(\boldsymbol{k}_3, \boldsymbol{k}_2)\} = 0, \quad \text{(A2)}$$

which is obvious if we use the fact $\sum_{\boldsymbol{k}} \propto \int d\boldsymbol{k}$. Here, the spin indices α and γ are omitted for notation simplicity. The above two equations show that the derivative operator $\bar{\partial}_{k_\mu}$ satisfies the Leibniz product rule,

$$\bar{\partial}_{k_\mu}(AB) = (\bar{\partial}_{k_\mu} A)B + A\bar{\partial}_{k_\mu} B. \quad \text{(A3)}$$

Besides, using the fact that $G_{i\omega} G_{i\omega}^{-1} = \mathbf{1}$ (for well defined G and G^{-1}), we have

$$\delta\left(G_{i\omega}\bar{\partial}_{k_\mu} G_{i\omega}^{-1}\right) = -G_{i\omega}\left(\bar{\partial}_{k_\mu} G_{i\omega}^{-1}\right)\delta G_{i\omega} G_{i\omega}^{-1} - (\bar{\partial}_{k_\mu}\delta G_{i\omega}) G_{i\omega}^{-1}. \quad \text{(A4)}$$

With these preparations, similar in the Ref. [76], it is not difficult to check that

$$\delta\chi[G_{i\omega}] \propto \epsilon^{\tilde{\mu}\tilde{\nu}\tilde{\rho}} \int d\omega \mathrm{Tr}\big[\bar{\partial}_{\tilde{\mu}}\big(G_{i\omega}^{-1}\delta G_{i\omega}\bar{\partial}_{\tilde{\nu}}G_{i\omega}^{-1}G_{i\omega}\bar{\partial}_{\tilde{\rho}}G_{i\omega}^{-1}G_{i\omega}\big)\big] = 0. \tag{A5}$$

Thus, χ is invariant under infinitesimal deformations of the Green's function, and therefore is a topological index. Note that the deduction requires well defined G and G^{-1}, which means the system is gapped at the Fermi energy.

APPENDIX B: HALL CONDUCTANCE IN THE EXTENDED INFINITE SYSTEM

The position $\boldsymbol{i}$ in the EIS can be expressed as $\boldsymbol{i} = \boldsymbol{R} + \boldsymbol{r}$, where $\boldsymbol{R}$ refers to the position of the corresponding supercell and $\boldsymbol{r}$ is the relative position in the supercell. For a general matrix A in real space, the translational symmetry implies the relation

$$A_{(\boldsymbol{R}+\boldsymbol{r})\alpha,(\boldsymbol{R}'+\boldsymbol{r}')\gamma} = A_{(\boldsymbol{R}-\boldsymbol{R}'+\boldsymbol{r})\alpha,\boldsymbol{r}'\gamma}. \tag{B1}$$

Using the Fourier transformation, in momentum space, we have

$$A_{\boldsymbol{k}\alpha,\boldsymbol{k}'\gamma} \equiv \frac{1}{N}\sum_{\boldsymbol{R}\boldsymbol{R}'\boldsymbol{r}\boldsymbol{r}'} A_{(\boldsymbol{R}+\boldsymbol{r})\alpha,(\boldsymbol{R}'+\boldsymbol{r}')\gamma} e^{i\boldsymbol{k}\cdot(\boldsymbol{R}+\boldsymbol{r})-i\boldsymbol{k}'\cdot(\boldsymbol{R}'+\boldsymbol{r}')}, \tag{B2}$$

for $k_\mu, k'_\mu \in [0, 2\pi)$ with $\mu = x, y$, where the lattice constant is set to be $a = 1$. The EIS retains the translational symmetry at a large scale, and the Bloch wave vector is denoted as $\theta_\mu \in [0, 2\pi/n_\mu)$, where $n_x \times n_y$ is the size of the supercell. Splitting the momenta as $k_\mu = \tilde{k}_\mu + \theta_\mu$ and $k'_\mu = \tilde{k}'_\mu + \theta'_\mu$, with $\tilde{k}_\mu = 2\pi l/n_\mu$ and $\tilde{k}'_\mu = 2\pi l'/n_\mu$ $(l, l' = 0, 1, \ldots, n_\mu - 1)$, and using the fact that $e^{i\tilde{\boldsymbol{k}}\cdot\boldsymbol{R}} = e^{i\tilde{\boldsymbol{k}}'\cdot\boldsymbol{R}'} = 1$, we obtain

$$A_{\boldsymbol{k}\alpha,\boldsymbol{k}'\gamma} = \frac{1}{N}\sum_{\boldsymbol{R}\boldsymbol{R}'\boldsymbol{r}\boldsymbol{r}'} A_{(\boldsymbol{R}-\boldsymbol{R}'+\boldsymbol{r})\alpha,\boldsymbol{r}'\gamma} e^{i\boldsymbol{\theta}\cdot(\boldsymbol{R}+\boldsymbol{r})-i\boldsymbol{\theta}'\cdot(\boldsymbol{R}'+\boldsymbol{r}')} e^{i\tilde{\boldsymbol{k}}\cdot\boldsymbol{r}-i\tilde{\boldsymbol{k}}'\cdot\boldsymbol{r}'}. \tag{B3}$$

Introducing new variables $\boldsymbol{R}_s \equiv \boldsymbol{R}'$ and $\boldsymbol{R}_a \equiv \boldsymbol{R} - \boldsymbol{R}'$, and using the fact that $\sum_{\boldsymbol{R}_s} e^{i(\boldsymbol{\theta}-\boldsymbol{\theta}')\cdot\boldsymbol{R}_s} = \frac{N}{n_x n_y}\delta_{\boldsymbol{\theta}\boldsymbol{\theta}'}$, we obtain

$$A_{(\tilde{\boldsymbol{k}}+\boldsymbol{\theta})\alpha,(\tilde{\boldsymbol{k}}'+\boldsymbol{\theta}')\gamma} = \frac{1}{n_x n_y}\sum_{\boldsymbol{R}_a\boldsymbol{r}\boldsymbol{r}'} A_{(\boldsymbol{R}_a+\boldsymbol{r})\alpha,\boldsymbol{r}'\gamma} e^{i\boldsymbol{\theta}\cdot(\boldsymbol{R}_a+\boldsymbol{r}-\boldsymbol{r}')} e^{i\tilde{\boldsymbol{k}}\cdot\boldsymbol{r}-i\tilde{\boldsymbol{k}}'\cdot\boldsymbol{r}'}\delta_{\boldsymbol{\theta}\boldsymbol{\theta}'}, \tag{B4}$$

so that we have

$$A_{\boldsymbol{k}\alpha,\boldsymbol{k}'\gamma} = A_{(\tilde{\boldsymbol{k}}+\boldsymbol{\theta})\alpha,(\tilde{\boldsymbol{k}}'+\boldsymbol{\theta})\gamma}\delta_{\boldsymbol{\theta}\boldsymbol{\theta}'}, \tag{B5}$$

which is exactly due to the translational symmetry. It also implies that

$$\bar{\partial}_\mu A_{\boldsymbol{k}\alpha,\boldsymbol{k}'\gamma} = [\partial_{\theta_\mu} A_{(\tilde{\boldsymbol{k}}+\boldsymbol{\theta})\alpha,(\tilde{\boldsymbol{k}}'+\boldsymbol{\theta})\gamma}]\delta_{\boldsymbol{\theta}\boldsymbol{\theta}'}. \tag{B6}$$

Let us define

$$A^{\boldsymbol{\theta}}_{\boldsymbol{r}\alpha,\boldsymbol{r}'\gamma} \equiv \sum_{\boldsymbol{R}} A_{(\boldsymbol{R}+\boldsymbol{r})\alpha,\boldsymbol{r}'\gamma} e^{i\boldsymbol{\theta}\cdot(\boldsymbol{R}+\boldsymbol{r}-\boldsymbol{r}')}, \tag{B7}$$

and then

$$A_{(\tilde{\boldsymbol{k}}+\boldsymbol{\theta})\alpha,(\tilde{\boldsymbol{k}}'+\boldsymbol{\theta})\gamma} = \frac{1}{n_x n_y}\sum_{\boldsymbol{r}\boldsymbol{r}'} A^{\boldsymbol{\theta}}_{\boldsymbol{r}\alpha,\boldsymbol{r}'\gamma} e^{i\tilde{\boldsymbol{k}}\cdot\boldsymbol{r}-i\tilde{\boldsymbol{k}}'\cdot\boldsymbol{r}'} \tag{B8}$$

is exactly the Fourier transformation of $A^{\boldsymbol{\theta}}_{\boldsymbol{r}\alpha,\boldsymbol{r}'\gamma}$ in a supercell.

In the following, we would like to show that $A^{\boldsymbol{\theta}}_{\boldsymbol{r}\alpha,\boldsymbol{r}'\gamma}$ is corresponding to the matrix with twist phases. Denote the right eigenvectors of $A^{\boldsymbol{\theta}}_{\boldsymbol{r}\alpha,\boldsymbol{r}'\gamma}$ as $\psi^{\boldsymbol{\theta}}$ with an eigenvalue E, then we have

$$\sum_{\boldsymbol{r}'\gamma} A^{\boldsymbol{\theta}}_{\boldsymbol{r}\alpha,\boldsymbol{r}'\gamma}\psi^{\boldsymbol{\theta}}_{\boldsymbol{r}'\gamma} = \sum_{\boldsymbol{R}'\boldsymbol{r}'\gamma} A_{(\boldsymbol{R}+\boldsymbol{r})\alpha,(\boldsymbol{R}'+\boldsymbol{r}')\gamma} e^{i\boldsymbol{\theta}\cdot(\boldsymbol{R}-\boldsymbol{R}'+\boldsymbol{r}-\boldsymbol{r}')}\psi^{\boldsymbol{\theta}}_{\boldsymbol{r}'\gamma} = E\psi^{\boldsymbol{\theta}}_{\boldsymbol{r}\alpha}, \tag{B9}$$

and thus

$$\sum_{\boldsymbol{R}'\boldsymbol{r}'\gamma} A_{(\boldsymbol{R}+\boldsymbol{r})\alpha,(\boldsymbol{R}'+\boldsymbol{r}')\gamma} e^{-i\boldsymbol{\theta}\cdot(\boldsymbol{R}'+\boldsymbol{r}')}\psi^{\boldsymbol{\theta}}_{\boldsymbol{r}'\gamma} = E e^{-i\boldsymbol{\theta}\cdot(\boldsymbol{R}+\boldsymbol{r})}\psi^{\boldsymbol{\theta}}_{\boldsymbol{r}\alpha}. \tag{B10}$$

So the corresponding eigenstates of $A_{(\boldsymbol{R}+\boldsymbol{r})\alpha,(\boldsymbol{R}'+\boldsymbol{r}')\gamma}$ become $\phi_{(\boldsymbol{R}+\boldsymbol{r})\alpha} \equiv e^{-i\boldsymbol{\theta}\cdot(\boldsymbol{R}+\boldsymbol{r})}\psi^{\boldsymbol{\theta}}_{\boldsymbol{r}\alpha}$, which shows the relation at the boundary of the supercell, $\phi_{(\boldsymbol{r}+n_\mu\hat{\mu})\alpha} = e^{-i\theta_\mu n_\mu}\phi_{\boldsymbol{r}\alpha}$. The phase $\theta_\mu n_\mu$ is an effective twisted phase boundary condition in the supercell.

Applying this definition (B7) for the Hamiltonian H_0, self-energy, and the Green's function, we find that $\Sigma^{\boldsymbol{\theta}}_{i\omega} = \Sigma_{i\omega}$ and $G^{\boldsymbol{\theta}}_{i\omega} = 1/(i\omega\mathbf{1} - H^{\boldsymbol{\theta}}_0 - \Sigma_{i\omega})$. After combining these results with Eqs. (B5)–(B8), the conductance Eq. (20) becomes

$$\sigma_H = \frac{\epsilon^{\tilde{\mu}\tilde{\nu}\tilde{\rho}}}{12\pi N}\int d\omega \sum_{\boldsymbol{\theta}} \mathrm{Tr}\big\{G^{\boldsymbol{\theta}}_{i\omega}\partial_{\tilde{\mu}}\big[G^{\boldsymbol{\theta}}_{i\omega}\big]^{-1}G^{\boldsymbol{\theta}}_{i\omega}\partial_{\tilde{\nu}}\big[G^{\boldsymbol{\theta}}_{i\omega}\big]^{-1}G^{\boldsymbol{\theta}}_{i\omega} \times \partial_{\tilde{\rho}}\big[G^{\boldsymbol{\theta}}_{i\omega}\big]^{-1}\big\}, \tag{B11}$$

where $\tilde{\mu}$, $\tilde{\nu}$, and $\tilde{\rho}$ run through θ_x, θ_y, and ω now and the trace is only for the supercell lattice and spin index. Using the fact that $\partial_{\tilde{\mu}}[G^{\boldsymbol{\theta}}_{i\omega}]^{-1} = -\partial_{\tilde{\mu}}H^{\boldsymbol{\theta}}_0$ for $\tilde{\mu} = \theta_x, \theta_y$ and $\partial_\omega[G^{\boldsymbol{\theta}}_{i\omega}]^{-1} = i\mathbf{1} - \partial_\omega\Sigma_{i\omega}$, and using the replacement $\frac{1}{N}\sum_{\boldsymbol{\theta}} = \frac{1}{4\pi^2}\int d\boldsymbol{\theta}$, we obtain $\sigma_H = \chi/2\pi$, where

$$\chi = \frac{\varepsilon^{\tilde{\mu}\tilde{\nu}}}{8\pi^2}\int d\omega d\boldsymbol{\theta}\mathrm{Tr}\big[G^{\boldsymbol{\theta}}_{i\omega}\big(\partial_{\tilde{\mu}}H^{\boldsymbol{\theta}}_0\big)G^{\boldsymbol{\theta}}_{i\omega}\big(\partial_{\tilde{\nu}}H^{\boldsymbol{\theta}}_0\big)G^{\boldsymbol{\theta}}_{i\omega}A_{i\omega}\big]. \tag{B12}$$

Here, $\tilde{\mu}$ and $\tilde{\nu}$ run through θ_x and θ_y now, and $A_{i\omega} = \partial_\omega[G^{\boldsymbol{\theta}}_{i\omega}]^{-1} = i\mathbf{1} - \partial_\omega\Sigma_{i\omega}$. The expression (B12) is exactly the Chern number of a periodic system with the Bloch momentum $\boldsymbol{\theta}$, and the site index in the supercell becomes an internal degree of freedom like a pseudospin. Our method is consistent with the proposal for the Chern number in a disordered system via introducing twisted phases for the Green's function [41].

APPENDIX C: WARD-TAKAHASHI IDENTITY

In this section, we derive the Ward-Takahashi identity in disordered systems, and prove that the vertex with full quantum corrections within (R)DMFT is consistent with the bare vertex.

For a general two-dimensional system in the continuous space, we write the Hermitian current operator as

$$\hat{j}^\mu(x) = \hat{c}^\dagger(x)\Gamma^\mu\hat{c}(x), \tag{C1}$$

where the bare vertex Γ^μ is a Hermitian matrix (and $\Gamma^0 = \mathbf{1}$ for the charge density $\hat{j}^0$). Here we use the convention $x = (x^1, x^2, x^0)$ for $2+1$-dimensional space-time. x^0 represents the real time. The position in two-dimensional space is denoted as $\boldsymbol{x} = (x^1, x^2)$. Here we consider the zero-temperature

limit ($\beta \to \infty$). The particle number operator satisfies the equal-time commutation relation

$$[\hat{j}^0(x), \hat{c}(y)]\delta(x^0 - y^0) = -\hat{c}(y)\delta^3(x-y), \tag{C2}$$

$$[\hat{j}^0(x), \hat{c}^\dagger(y)]\delta(x^0 - y^0) = \hat{c}^\dagger(y)\delta^3(x-y), \tag{C3}$$

where $\delta^3(x-y) \equiv \delta(x^1-y^1)\delta(x^2-y^2)\delta(x^0-y^0)$. The continuity equation in Heisenberg picture is

$$\partial_{x^\mu}\hat{j}^\mu(x) = 0, \tag{C4}$$

which represents the charge conservation due to the U(1) symmetry. Here the Einstein summation convention is used. The metric matrix for the space-time is $g = \mathrm{diag}(1, 1, -1)$. The above three equations also work for the imaginary time $x^0 = -i\tau$. This is obvious for Eqs. (C2) and (C3). In the following, we prove that Eq. (C4) works for the imaginary time. For the real time $x^0 = t$, we can rewrite Eq. (C4) as

$$\partial_t \hat{j}^0(\boldsymbol{x}, t) = -\boldsymbol{\nabla}\cdot\hat{\boldsymbol{j}}(\boldsymbol{x}, t). \tag{C5}$$

Using the definition $\hat{j}^0(\boldsymbol{x}, t) \equiv e^{it\hat{H}}\hat{j}^0(\boldsymbol{x}, 0)e^{-it\hat{H}}$, we have the following relation:

$$i[\hat{H}, \hat{j}^0(\boldsymbol{x}, 0)] = -\boldsymbol{\nabla}\cdot\hat{\boldsymbol{j}}(\boldsymbol{x}, 0). \tag{C6}$$

Thus for $\hat{j}^0(\boldsymbol{x}, \tau) \equiv e^{\tau\hat{H}}\hat{j}^0(\boldsymbol{x}, 0)e^{-\tau\hat{H}}$, we also have Eq. (C4) with ∂_t replaced by $\partial_{-i\tau}$.

In the following, we would like to derive the Ward-Takahashi identity in imaginary time space (i.e., $x^0 = -i\tau$) for a disordered system. Equations (C2)–(C4) imply the following relation:

$$\begin{aligned}&\partial_{x^\mu}\langle T_\tau \hat{j}^\mu(x)\hat{c}(y)\hat{c}^\dagger(z)\rangle \\ &\quad = -i\langle T_\tau \hat{c}(y)\hat{c}^\dagger(z)\rangle\{\tilde{\delta}^3(x-y) - \tilde{\delta}^3(x-z)\}.\end{aligned} \tag{C7}$$

Here in imaginary time space, we use the conventions $\tilde{\delta}^3(x-y) \equiv \delta(x^1-y^1)\delta(x^2-y^2)\delta(ix^0-iy^0)$, $d^3x = idx^1dx^2dx^0$, $p = (p^1, p^2, p^0 = i\omega)$, and $d^3p = dp^1dp^2d\omega$. For a disordered system, the impurity violates the translational symmetry. We use the Fourier transformation to obtain the momentum representation for the Green's function,

$$\begin{aligned}&\int d^3x d^3y e^{-i(p'x-py)}\langle T_\tau \hat{c}(x)\hat{c}^\dagger(y)\rangle \\ &\quad = -(2\pi)^3\delta(ip'^0 - ip^0)G_{p^0}(\boldsymbol{p}', \boldsymbol{p}),\end{aligned} \tag{C8}$$

where $p'x \equiv p'_\mu x^\mu$ and all internal degrees of freedom (such as spin) are hidden. Note that the Green's function is not diagonal in momentum space due to the disorder. The delta function here is due to the energy conservation. The factor $(2\pi)^3$ comes from the fact that $\hat{c}(x) = \frac{1}{(2\pi)^{3/2}}\int d^3p e^{ipx}\hat{c}(p)$. Similarly, we have

$$\begin{aligned}&\int d^3x d^3y d^3z e^{-i(p'y-pz-qx)}\langle T_\tau \hat{j}^\mu(x)\hat{c}(y)\hat{c}^\dagger(z)\rangle \\ &\quad = (2\pi)^3\delta(ip'^0 - ip^0 - iq^0)\sum_{\boldsymbol{k},\boldsymbol{k}'} G_{p'^0}(\boldsymbol{p}', \boldsymbol{k}')\Lambda^\mu_{q,p^0}(\boldsymbol{k}', \boldsymbol{k}) \\ &\qquad \times G_{p^0}(\boldsymbol{k}, \boldsymbol{p}),\end{aligned} \tag{C9}$$

where Λ^μ is the dressed vertex with full quantum corrections [it represents a vertex with one ingoing particle with $(\boldsymbol{k}', p^0 + q^0)$, one outgoing particle with $(\boldsymbol{k}, p^0)$, and one outgoing gauge field with $q \equiv (\boldsymbol{q}, q^0)$]. Using partial integration, we have

$$\begin{aligned}&\int d^3x d^3y d^3z e^{-i(p'y-pz-qx)}\partial_{x^\mu}\langle T_\tau \hat{j}^\mu(x)\hat{c}(y)\hat{c}^\dagger(z)\rangle \\ &\quad = -(2\pi)^3 iq_\mu\delta(ip'^0 - ip^0 - iq^0)\sum_{\boldsymbol{k},\boldsymbol{k}'} G_{p'^0}(\boldsymbol{p}', \boldsymbol{k}') \\ &\qquad \times \Lambda^\mu_{q,p^0}(\boldsymbol{k}', \boldsymbol{k})G_{p^0}(\boldsymbol{k}, \boldsymbol{p}),\end{aligned} \tag{C10}$$

and then using Eqs. (C7) and (C8), we obtain

$$\begin{aligned}&-q_\mu\sum_{\boldsymbol{k},\boldsymbol{k}'} G_{p'^0}(\boldsymbol{p}', \boldsymbol{k}')\Lambda^\mu_{q,p^0}(\boldsymbol{k}', \boldsymbol{k})G_{p^0}(\boldsymbol{k}, \boldsymbol{p}) \\ &\quad = G_{p^0}(\boldsymbol{p}' - \boldsymbol{q}, \boldsymbol{p}) - G_{p'^0}(\boldsymbol{p}', \boldsymbol{p} + \boldsymbol{q}),\end{aligned} \tag{C11}$$

where $p'^0 = p^0 + q^0$. By left and right multiplying the inverse of the Green's function to Eq. (C11), we find the Ward-Takahashi identity of the disordered system,

$$-q_\mu\Lambda^\mu_{q,p^0}(\boldsymbol{p}', \boldsymbol{p}) = G^{-1}_{p'^0}(\boldsymbol{p}', \boldsymbol{p}+\boldsymbol{q}) - G^{-1}_{p^0}(\boldsymbol{p}'-\boldsymbol{q}, \boldsymbol{p}). \tag{C12}$$

Thus for $q = (\boldsymbol{q}, q^0) \to (\boldsymbol{0}, 0)$, we have

$$\Lambda^\mu_{q=0,p^0}(\boldsymbol{p}', \boldsymbol{p}) = -\bar{\partial}_\mu G^{-1}_{p^0}(\boldsymbol{p}', \boldsymbol{p}) \quad \text{for } \mu = 1, 2; \tag{C13}$$

$$\Lambda^0_{q=0,p^0}(\boldsymbol{p}', \boldsymbol{p}) = \partial_{p^0} G^{-1}_{p^0}(\boldsymbol{k}', \boldsymbol{p}); \tag{C14}$$

Here, $\bar{\partial}_\mu A(\boldsymbol{p}', \boldsymbol{p}) \equiv (\partial_{p'^\mu} + \partial_{p^\mu})A(\boldsymbol{p}', \boldsymbol{p})$. The change of the sign in Eq. (C14) occurs when lowering the index. As we have shown in the main text, within (R)DMFT, $-\bar{\partial}_\mu G^{-1}_{p^0}(\boldsymbol{p}', \boldsymbol{p})$ is exactly the bare vertex j^μ (for lattice structure, an additional factor $1/\sqrt{N}$ is introduced). Thus, the vertex with full quantum corrections within (R)DMFT is consistent with the bare vertex.

APPENDIX D: EFFECTIVE-MEDIUM THEORY

In the following, we derive the self-energy of a system with weak disorder and interaction, within the framework of the effective-medium theory. The averaged Green's function over different disorder samples can be written as

$$\overline{G}(\omega) \equiv \langle\langle G(\{V_i\}, \omega)\rangle\rangle = \frac{1}{\omega - h_0 - \overline{\Sigma}}, \tag{D1}$$

where $\langle\langle\mathcal{O}\rangle\rangle$ means the averaged result of $\mathcal{O}$ over different disorder samples. Given a sample of disorder $\{V_i\}$, the Green's function is denoted as

$$G(\{V_i\}, \omega) \equiv \frac{1}{G_0^{-1} - V - \Sigma^{\mathrm{U}}}. \tag{D2}$$

Here, $G_0 = 1/(\omega - h_0)$ is the free Green's function without disorder and interaction, and $\Sigma^{\mathrm{U}}_{i\alpha,j\gamma} \equiv U\langle\hat{c}_{i\alpha}\hat{c}^\dagger_{i\bar{\alpha}}\rangle\delta_{ij}\delta_{\bar{\alpha}\gamma} + U\langle\hat{c}^\dagger_{i\bar{\alpha}}\hat{c}_{i\bar{\alpha}}\rangle\delta_{ij}\delta_{\alpha\gamma}$ is the self-energy within the Hartree-Fock approximation for the weakly interacting case. The matrix V refers to the disorder potential, with elements $V_{ij} = V_i\delta_{ij}$.

The averaged Green's function can be evaluated by expanding the formula (D2) up to the order of W^2 and U. Then we have

$$\begin{aligned}\langle\langle G(\{V_i\}, \omega)\rangle\rangle = [1 &+ G_0\langle\langle V\rangle\rangle + G_0\langle\langle\Sigma^{\mathrm{U}}\rangle\rangle \\ &+ G_0\langle\langle V G_0 V\rangle\rangle]G_0(\omega).\end{aligned} \tag{D3}$$

Denoting $\overline{\Sigma}^{\mathrm{U}} \equiv \langle\langle \Sigma^{\mathrm{U}} \rangle\rangle$ and using the fact that $\langle\langle V \rangle\rangle = 0$ for the random events governed by the uniform distribution in $[-W, W]$, we get

$$\overline{G}^{-1}(\omega) = G_0^{-1}(\omega)[1 - G_0\overline{\Sigma}^{\mathrm{U}} - G_0\langle\langle V G_0 V \rangle\rangle]. \tag{D4}$$

According the definition of the self-energy (D1) in the effective-medium theory, we find

$$\overline{\Sigma} = \overline{\Sigma}^{\mathrm{U}} + \langle\langle V G_0 V \rangle\rangle. \tag{D5}$$

Since the disorder potential at different positions is independent, we have $\langle\langle V_i V_j \rangle\rangle = \delta_{ij} W^2/3$ for the uniform probability distribution. Finally, we get

$$\overline{\Sigma}_{ij} = \delta_{ij}\left\{\overline{\Sigma}_{ii}^{U} + G_{0,ii}\left\langle\left\langle V_i^2 \right\rangle\right\rangle\right\}. \tag{D6}$$

Note that the averaged Hartree-Fock self-energy $\overline{\Sigma}_{ii}^{U}$ can be obtained by evaluating the averaged value of the local operators $\hat{c}_{i\alpha}\hat{c}_{i\bar{\alpha}}^{\dagger}$ and $\hat{c}_{i\bar{\alpha}}^{\dagger}\hat{c}_{i\bar{\alpha}}$. These quantities can be calculated by using the effective Hamiltonian, $H_{\mathrm{eff}} = h_0 + \overline{\Sigma}$. The Green's function G_0 in Eq. (D6) can also be replaced by $\overline{G}$. The difference of the final results is of higher order.

[1] D. C. Tsui, H. L. Stormer, and A. C. Gossard, Phys. Rev. Lett. **48**, 1559 (1982).
[2] B. Huckestein, Rev. Mod. Phys. **67**, 357 (1995).
[3] P. A. Lee and T. V. Ramakrishnan, Rev. Mod. Phys. **57**, 287 (1985).
[4] B. Kramer and A. MacKinnon, Rep. Prog. Phys. **56**, 1469 (1993).
[5] Yu. G. Arapov, S. V. Gudina, V. N. Neverov, S. M. Podgornykh, M. R. Popov, G. I. Harus, N. G. Shelushinina, M. V. Yakunin, N. N. Mikhailov, and S. A. Dvoretsky, Semiconductors **49**, 1545 (2015).
[6] C. Wu, B. A. Bernevig, and S.-C. Zhang, Phys. Rev. Lett. **96**, 106401 (2006).
[7] C. Xu and J. E. Moore, Phys. Rev. B **73**, 045322 (2006).
[8] M. Hohenadler and F. F. Assaad, J. Phys.: Condens. Matter **25**, 143201 (2013).
[9] T. Neupert, L. Santos, C. Chamon, and C. Mudry, Phys. Rev. Lett. **106**, 236804 (2011).
[10] A. Ström, H. Johannesson, and G. I. Japaridze, Phys. Rev. Lett. **104**, 256804 (2010).
[11] F. Crépin, J. C. Budich, F. Dolcini, P. Recher, and B. Trauzettel, Phys. Rev. B **86**, 121106 (2012).
[12] F. Geissler, F. Crépin, and B. Trauzettel, Phys. Rev. B **89**, 235136 (2014).
[13] T. S. Nunner, G. Zaránd, and F. von Oppen, Phys. Rev. Lett. **100**, 236602 (2008).
[14] J.-H. Zheng and M. A. Cazalilla, Phys. Rev. B **97**, 235402 (2018).
[15] D. N. Sheng and Z. Y. Weng, Phys. Rev. Lett. **78**, 318 (1997).
[16] Y.-F. Zhang, Y.-Y. Yang, Y. Ju, L. Sheng, R. Shen, D.-N. Sheng, and D. Y. Xing, Chin. Phys. B **22**, 117312 (2013).
[17] S. Raghu, X.-L. Qi, C. Honerkamp, and S.-C. Zhang, Phys. Rev. Lett. **100**, 156401 (2008).
[18] A. Dauphin, M. Müller, and M. A. Martin-Delgado, Phys. Rev. A **93**, 043611 (2016).
[19] T. I. Vanhala, T. Siro, L. Liang, M. Troyer, A. Harju, and P. Törmä, Phys. Rev. Lett. **116**, 225305 (2016).
[20] L. Wang, X. Dai, and X. C. Xie, Europhys. Lett. **98**, 57001 (2012).
[21] P. Kumar, T. Mertz, and W. Hofstetter, Phys. Rev. B **94**, 115161 (2016).
[22] J. Li, R.-L. Chu, J. K. Jain, and S.-Q. Shen, Phys. Rev. Lett. **102**, 136806 (2009).
[23] C. W. Groth, M. Wimmer, A. R. Akhmerov, J. Tworzydlo, and C. W. J. Beenakker, Phys. Rev. Lett. **103**, 196805 (2009).
[24] R. Nakai and K. Nomura, Phys. Rev. B **89**, 064503 (2014).
[25] B. Wu, J. Song, J. Zhou, and H. Jiang, Chin. Phys. B **25**, 117311 (2016).
[26] C. P. Orth, T. Sekera, C. Bruder, and T. L. Schmidt, Sci. Rep. **6**, 24007 (2016).
[27] R. Chen, D.-H. Xu, and B. Zhou, Phys. Rev. B **96**, 205304 (2017).
[28] C.-Z. Chen, J. Song, H. Jiang, Q.-f. Sun, Z. Wang, and X. C. Xie, Phys. Rev. Lett. **115**, 246603 (2015).
[29] S. Liu, T. Ohtsuki, and R. Shindou, Phys. Rev. Lett. **116**, 066401 (2016).
[30] P. Titum, N. H. Lindner, M. C. Rechtsman, and G. Refael, Phys. Rev. Lett. **114**, 056801 (2015).
[31] P. Titum, E. Berg, M. S. Rudner, G. Refael, and N. H. Lindner, Phys. Rev. X **6**, 021013 (2016).
[32] H.-Z. Lu, J. Shi, and S.-Q. Shen, Phys. Rev. Lett. **107**, 076801 (2011).
[33] C.-K. Chiu, J. C. Y. Teo, A. P. Schnyder, and S. Ryu, Rev. Mod. Phys. **88**, 035005 (2016).
[34] X. G. Wen and Q. Niu, Phys. Rev. B **41**, 9377 (1990).
[35] D. J. Thouless, M. Kohmoto, M. P. Nightingale, and M. den Nijs, Phys. Rev. Lett. **49**, 405 (1982).
[36] Q. Niu, D. J. Thouless, and Y. S. Wu, Phys. Rev. B **31**, 3372 (1985).
[37] D. N. Sheng, Z. Y. Weng, L. Sheng, and F. D. M. Haldane, Phys. Rev. Lett. **97**, 036808 (2006); D. N. Sheng, L. Balents, and Z. Wang, *ibid.* **91**, 116802 (2003).
[38] S.-S. Lee and S. Ryu, Phys. Rev. Lett. **100**, 186807 (2008).
[39] T. A. Loring and M. B. Hastings, Europhys. Lett. **92**, 67004 (2010).
[40] K. Ishikawa and T. Matsuyama, Nucl. Phys. B **280**, 523 (1987).
[41] Z. Wang, X.-L. Qi, and S.-C. Zhang, Phys. Rev. Lett. **105**, 256803 (2010).
[42] A. M. Essin and V. Gurarie, J. Phys. A: Math. Theor. **48**, 11FT01 (2015).
[43] A. Georges, G. Kotliar, W. Krauth, and M. J. Rozenberg, Rev. Mod. Phys. **68**, 13 (1996).
[44] Jairo Sinova, A. H. MacDonald, and S. M. Girvin, Phys. Rev. B **62**, 13579 (2000).
[45] D. Makogon, A. Alamir, and C. M. Smith, Phys. Rev. B **81**, 045310 (2010).
[46] P. M. Ostrovsky, I. V. Gornyi, and A. D. Mirlin, Phys. Rev. Lett. **105**, 036803 (2010).
[47] J. Wang, C. Ortix, J. van den Brink, and D. V. Efremov, Phys. Rev. B **96**, 201104(R) (2017).
[48] F. Evers and A. D. Mirlin, Rev. Mod. Phys. **80**, 1355 (2008).

[49] H.-H. Hung, A. Barr, E. Prodan, and G. A. Fiete, Phys. Rev. B **94**, 235132 (2016).
[50] K. Byczuk, W. Hofstetter, and D. Vollhardt, Phys. Rev. Lett. **94**, 056404 (2005).
[51] D. Semmler, K. Byczuk, and W. Hofstetter, Phys. Rev. B **84**, 115113 (2011).
[52] Y. Hatsugai and M. Kohmoto, Phys. Rev. B **42**, 8282 (1990).
[53] B. A. Bernevig and T. L. Hughes, *Topological Insulators and Topological Superconductors* (Princeton University Press, Princeton, NJ, 2013), Chap. 3.
[54] G. D. Mahan, *Many-Particle Physics* (Kluwer Academic/ Plenum Publisher, New York, 2000).
[55] M. Snoek, I. Titvinidze, C. Töke, K. Byczuk, and W. Hofstetter, New J. Phys. **10**, 093008 (2008).
[56] H. Kohno and K. Yamada, Prog. Theor. Phys. **80**, 623 (1988).
[57] H. Park, K. Haule, and G. Kotliar, Phys. Rev. Lett. **101**, 186403 (2008).
[58] D. Ceresoli and R. Resta, Phys. Rev. B **76**, 012405 (2007).
[59] Y.-Y. Zhang, R.-L. Chu, F.-C. Zhang, and S.-Q. Shen, Phys. Rev. B **85**, 035107 (2012).
[60] R. Shindou and L. Balents, Phys. Rev. Lett. **97**, 216601 (2006); Phys. Rev. B **77**, 035110 (2008).
[61] J.-H. Zheng and W. Hofstetter, Phys. Rev. B **97**, 195434 (2018).
[62] H. Kajueter and G. Kotliar, Phys. Rev. Lett. **77**, 131 (1996).
[63] M. Potthoff, T. Wegner, and W. Nolting, Phys. Rev. B **55**, 16132 (1997).
[64] D. Semmler, J. Wernsdorfer, U. Bissbort, K. Byczuk, and W. Hofstetter, Phys. Rev. B **82**, 235115 (2010).
[65] K. Byczuk, W. Hofstetter, and D. Vollhardt, Phys. Rev. Lett. **102**, 146403 (2009).
[66] S. S. Kondov, W. R. McGehee, W. Xu, and B. DeMarco, Phys. Rev. Lett. **114**, 083002 (2015).
[67] S. Nakajima, T. Tomita, S. Taie, T. Ichinose, H. Ozawa, L. Wang, M. Troyer, and Y. Takahashi, Nat. Phys. **12**, 296 (2016).
[68] M. Lohse, C. Schweizer, O. Zilberberg, M. Aidelsburger, and I. Bloch, Nat. Phys. **12**, 350 (2016).
[69] B. Damski, J. Zakrzewski, L. Santos, P. Zoller, and M. Lewenstein, Phys. Rev. Lett. **91**, 080403 (2003).
[70] J. E. Lye, L. Fallani, M. Modugno, D. S. Wiersma, C. Fort, and M. Inguscio, Phys. Rev. Lett. **95**, 070401 (2005).
[71] D. Clément, A. F. Varón, M. Hugbart, J. A. Retter, P. Bouyer, L. Sanchez-Palencia, D. M. Gangardt, G. V. Shlyapnikov, and A. Aspect, Phys. Rev. Lett. **95**, 170409 (2005).
[72] D. Clément, A. Varon, J. Retter, L. Sanchez-Palencia, A. Aspect, and P. Bouyer, New J. Phys. **8**, 165 (2006).
[73] M. White, M. Pasienski, D. McKay, S. Q. Zhou, D. Ceperley, and B. DeMarco, Phys. Rev. Lett. **102**, 055301 (2009).
[74] E. J. Meier, F. A. An, A. Dauphin, M. Maffei, P. Massignan, T. L. Hughes, and B. Gadway, Science **362**, 929 (2018).
[75] M. Aidelsburger, M. Lohse, C. Schweizer, M. Atala, J. T. Barreiro, S. Nascimbène, N. R. Cooper, I. Bloch, and N. Goldman, Nat. Phys. **11**, 162 (2015).
[76] X.-L. Qi, T. L. Hughes, and S.-C. Zhang, Phys. Rev. B **78**, 195424 (2008).